Artificial Organs

Copyright © 2017 International Center for Artificial Organs and Transplantation and Wiley Periodicals, Inc.

Review Article

Evolution of Gas Permeable Membranes for Extracorporeal Membrane Oxygenation

Torin Yeager and Shuvo Roy

Department of Bioengineering and Therapeutic Sciences, University of California, San Francisco, CA, USA

Abstract: Gas permeable membranes are a vital component of extracorporeal membrane oxygenation systems. Over more than half a century, membrane fabrication and packaging technology have progressed to enable safer and longer duration use of respiratory life support. Current research efforts seek to improve membrane efficiency and hemocompatibility, with the aim of producing smaller and more robust systems for ambulatory use. This review explores past and present innovations in oxygenator technology, suggesting possible applications of state-of-the-art membrane fabrication methods to address shortcomings of earlier concepts. **Key Words:** Extracorporeal membrane oxygenation—Extracorporeal life support—Gas exchange—Membrane.

Extracorporeal membrane oxygenation (ECMO) is a life support method used to oxygenate blood and ventilate carbon dioxide without the need for functioning native lungs. In its simplest form, venous blood with low oxygen and elevated carbon dioxide content is withdrawn from the patient, flowed across a membrane oxygenator to exchange oxygen and carbon dioxide between the blood and a sweep gas, and then returned to the body (1,2). ECMO is capable of maintaining healthy organ function, allowing a patient to survive and heal from cardiopulmonary surgery, traumatic injury, infection, or inflammation of the lungs over periods of hours to weeks. ECMO is also used as a bridge to lung transplant (3,4), allowing patients to maintain stable blood gas levels and, perhaps equally importantly, to remain awake and ambulatory (5,6) while awaiting a donor organ. ECMO technology has advanced considerably since the earliest development on artificial lungs began in the 1930s (7), including revolutionary and evolutionary improvements in blood pumps, tubing, gas exchangers, and surgical practices. This review will focus on the evolution of the core component of modern ECMO, the oxygenator membrane, and the future of this technology. As summarized in Table 1, oxygenators have progressed from exposed blood films, to sandwiched parallel membrane arrays, to dialyzer-like hollow fibers, to microfluidic capillary systems that mimic the physiology of the alveoli in the native lung. All of these technologies, with their inherent strengths and weaknesses, have made vital contributions to the field of extracorporeal life support that can inform future oxygenator designs.

EARLY DEVELOPMENT OF GAS EXCHANGE MEMBRANES: 1950s–1960s

The first successful cardiopulmonary bypass was performed on a human patient in 1954 by John Gibbon, Jr. (8). Venous blood was drained from the patient using finger cot pumps and cascaded down a rotating cylinder. The centrifugal force exerted on the blood caused it to spread into a thin film on the interior surface of the cylinder, where it was directly exposed to an oxygen-rich atmosphere, as shown in Fig. 1; fully oxygenated blood was returned through an arterial cannula. The product of more than two decades of development (7), the heart-lung machine was designed to provide gas

doi: 10.1111/aor.12835

Received June 2016; revised August 2016; accepted August 2016.

Address correspondence and reprint requests to Shuvo Roy, Department of Bioengineering and Therapeutic Sciences, University of California, 1700 4th St BH 203, San Francisco, CA 94158, USA. E-mail: shuvo.roy@ucsf.edu

TABLE 1. *Summary of technical and clinical milestones in ECMO*

Year	ECMO milestone	Reference(s)
1954	First cardiopulmonary bypass, using blood film directly exposed to atmosphere	(7,8)
1955	Blood oxygenation demonstrated using sheets of polymer membrane between blood and sweep gas (parallel plate oxygenator)	(9,10)
Early 1970s	Introduction of hollow fiber oxygenators, derived from renal dialyzers	(11)
1972	First successful clinical use of ECMO	(12)
Mid 1980s	Development of hollow fiber oxygenators with extraluminal "cross-flow" of blood	(13)
Late 1990s–present	Research begins on microfluidic oxygenators	(14–16)

exchange while open heart surgery was performed, typically lasting less than 1 h. This groundbreaking system informed much of the preliminary work in extracorporeal life support.

As had been witnessed earlier by Gibbon and colleagues, researchers seeking to develop new oxygenators found that direct exposure of blood to atmosphere, whether in a rotating cylinder, rotating disc (17), screen cascade (18), or bubbling system (19), would cause foaming of the blood. The foaming action led to blood trauma and loss of blood products during and following oxygenator usage (19,20). While brief atmospheric exposure could be accommodated during cardiopulmonary bypass, the rapid consumption of blood products and risk of arterial gas emboli during life support sessions greater than several hours generated demand for new oxygenator designs.

Seeking to eliminate the blood-gas interface in oxygenators, Clowes and colleagues performed pioneering work in the use of plastic sheets for gas transfer in a parallel plate, or sandwich, geometry (9). Several plastic films were tested as diffusion membranes between a pure oxygen supply at 760 mm Hg and a reservoir of continuously mixed blood. One such polyethylene film, of 25 μm thickness, was capable of transferring 11.2 mL O_2 m^{-2} min^{-1}; although thinner polyethylene films were capable of higher gas exchange, contemporary manufacturing techniques produced pinhole defects that allowed oxygen bubbles to enter the blood channel (9). Clowes later demonstrated successful oxygenation via diffusion through 25 μm thick ethylcellulose membranes in a 6 m^2 stacked parallel plate system (10), providing oxygen exchange of 14.6 mL O_2 m^{-2} min^{-1}. However, ethylcellulose allowed water to seep into the gas channel, and the brittle material was difficult to support mechanically. The pressure of the sweep gas was used to control the separation distance between two plates and adjust the height of adjoining blood channels, but excessive gas pressure often resulted in emboli in the blood channel.

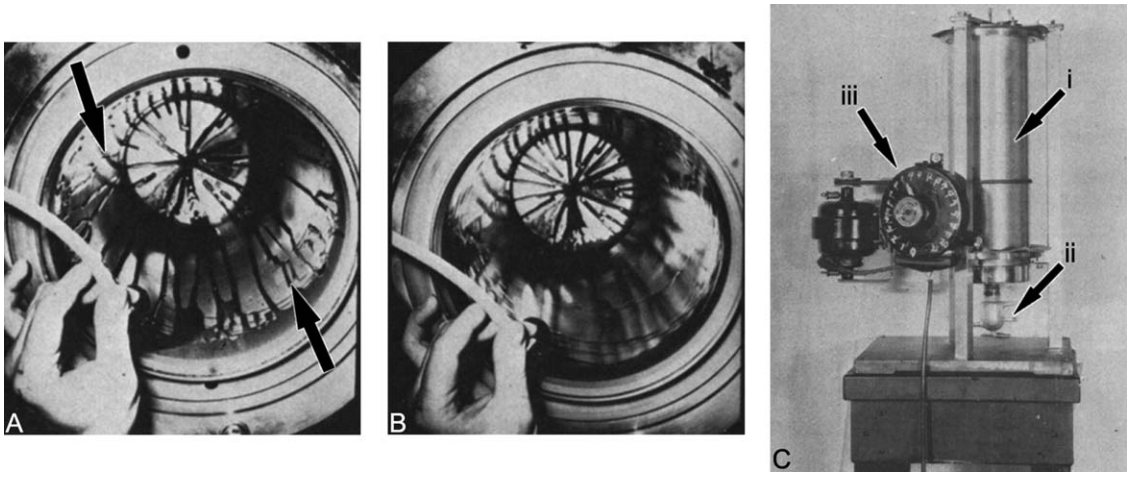

FIG. 1. Gibbon blood film oxygenator. (A) Blood flowing down the cylinder in rivulets (indicated by arrows) when the cylinder was stationary. (B) Blood film produced by rotating the cylinder. (C) The first oxygenator used, showing the revolving cylinder (i) and the stationary cup (ii) at the bottom that returned blood to the patient. The rheostat (iii) controlled the rate of revolution of the cylinder. Adapted from Gibbon (7).

While contemporary artificial lungs relied on Teflon and silicone rubber in flat sheets or tubes due to availability of preexisting industrial materials, in 1969 Galletti and colleagues proposed that blood flow could be more closely controlled by machining capillary channels into the membrane sheets (21). A parallel capillary channel pattern could be imprinted on a microporous substrate by rollers, then skinned with a 10 μm thick silicone film; such silicone-coated fabric sheets were suggested to provide mechanical strength to thin but fragile membranes (22). Technical challenges that could not be adequately addressed at the time included maintaining the desired plate separation, which allowed blood shunting to poorly oxygenated regions, and water condensation on the microporous substrate that limited gas exchange.

In order to overcome material defects and resulting gas embolism in 76 μm thick silicone films supported by Dacron and fiberglass meshes, Kolobow and colleagues employed a hypobaric oxygen sweep gas (23) in a spiral-wound parallel plate membrane oxygenator, as shown in Fig. 2. Blood could then leak through any membrane holes into the lower pressure sweep gas chamber, rather than allowing gas bubbles to infiltrate the blood channel. This improved the safety of the device at the cost of a decreased oxygen partial pressure gradient across the membrane; using a membrane surface area of 1.2 m^2 with sweep O_2 pressure of 500 mm Hg provided a gas transfer rate of 82 mL O_2 m^{-2} min^{-1}. Since the oxygenator did not feature fixed structural supports in the blood channel, the channel height could be dynamically varied around a mean height of 80 microns by fluctuating the sweep gas pressure, which mixed the blood and improved gas exchange when compared to static channels. Later developments enabled the coating of 13 μm silicone rubber on microporous fabric substrates to provide greater gas transfer (22).

Despite the promising gas exchange performance of the early membranes, the manufacturing processes were not yet optimized, resulting in inconsistent performance (9). Clinical adoption was also limited by the time consuming preparation and cleaning processes required for operation and reuse of oxygenators.

PARALLEL PLATE OPTIMIZATIONS AND THE RISE OF CLINICAL ECMO: 1960s–1970s

In an effort to produce a clinically useable membrane oxygenator, the Bramson lung was developed as a 6 m^2 parallel plate system comprised of 15 individually transfused blood channels, shown in Fig. 3. The blood channel was enveloped by 51 μm thick reinforced silicone sheets to form concentric gas and water chambers, which oxygenated and heated the blood, respectively (24,25). The surrounding water chamber had the added benefit of compressing the plates to control blood channel height without requiring adjustment of sweep gas pressure.

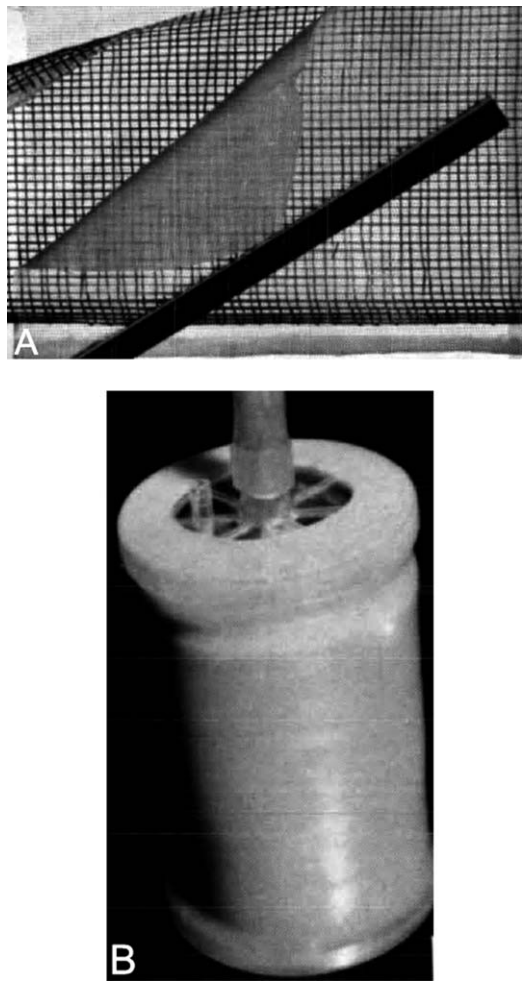

FIG. 2. Kolobow cylindrical oxygenator. (A) Silastic-coated Dacron screen with fiberglass supporting screen used for gas exchange membrane. (B) Assembled cylinder oxygenator consisting of wrapped layers of silastic-coated Dacron and fiberglass. Adapted from Kolobow (23).

A similar clinically scaled device, the Landé-Edwards oxygenator, shown in Fig. 4, utilized silicone copolymer membrane sheets to form a stack of 58 parallel plates with 3 m^2 total membrane area (26–28). Blood channel height was controlled using corrugation of the membrane sheets by a grooved plastic support wafer to define 1440 capillary channels per plate, with a 3 cm blood path length (28).

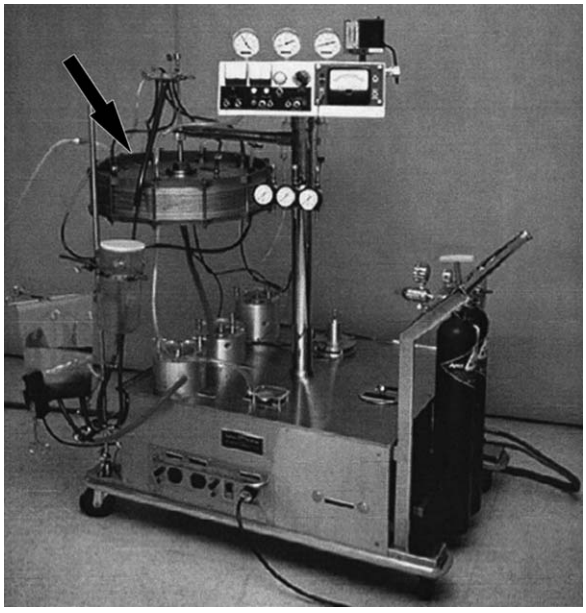

FIG. 3. Bramson membrane heart-lung machine, adapted from Schulte (25). The stacked parallel plate oxygenator, with total surface area of 6 m^2, is indicated by the arrow.

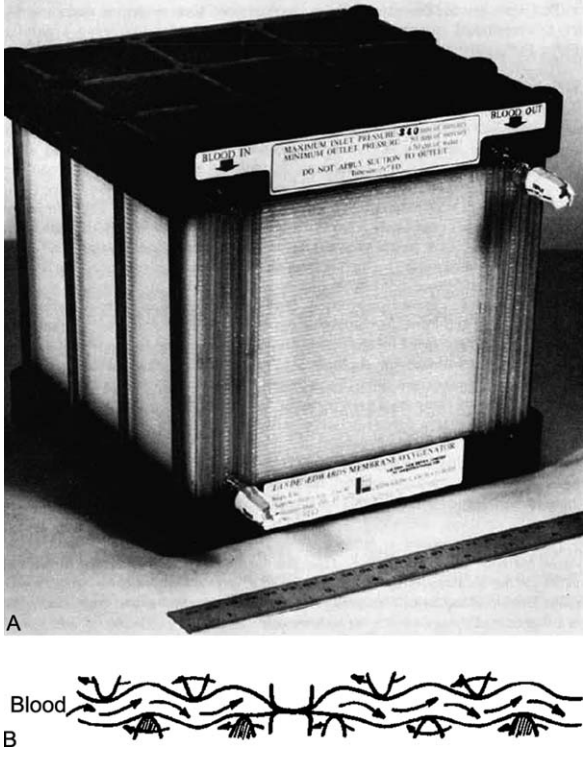

FIG. 4. (A) Landé-Edwards parallel plate oxygenator assembled from folded silicone membrane sheets with 3 m^2 total area, reproduced from Carlson (28). (B) Diagram of blood flow between membrane layers supported by corrugated plastic structure. The change in direction of blood flow was designed to induce mild non-turbulent mixing of the blood layer; reproduced from Landé (26).

Pulsatile modulation of the sweep gas pressure was used to vary the blood layer thickness between 76 and 127 μm and promote mixing. The design avoided costly and difficult assembly of small membrane sections by pleating a single large membrane sheet to form a stack of alternating blood and gas channels (26); multiple oxygenators could be used in parallel to form a modular life support system for larger patients. The preassembled oxygenator was also disposable, greatly simplifying setup for clinical procedures.

Due in part to the large (150–1500 μm) plate separation distances imposed by manufacturing technology at the time, Gaylor and Mockros determined that parallel plate oxygenators incorporating woven nylon mesh screens in the blood channel could surpass the performance of open blood channels (29). While the mesh screens roughly doubled the total foreign material surface area in contact with blood, the interruption of blood flow induced turbulent mixing to greatly enhance the rate of gas exchange and reduce the required membrane area by approximately half. These features provided the advantage of smaller oxygenators with lower priming volume, while the mesh also served as a structural support to maintain the membrane plate separation. This design was employed commercially in the Travenol oxygenator, shown in Fig. 5.

Planar parallel plate oxygenators such as the Bramson or Landé-Edwards, mesh screen-supported plate oxygenators such as the Travenol (30), and commercial variants of Kolobow-type spiral oxygenators were of particular interest to clinicians due to their disposable nature. Rather than requiring costly and time consuming cleaning and reassembly of membranes, which had led many clinicians to continue using less expensive and easier to prepare bubble oxygenators (31), the relatively simple construction encouraged the wider adoption of membrane oxygenators.

The first successful long-duration use of ECMO to support a human patient was reported in 1972 (12), using a Bramson oxygenator to enable recovery from "shock lung," or acute respiratory distress syndrome, over a period of 75 h. Meanwhile, ECMO support of neonatal and pediatric patients was performed by Bartlett and colleagues using Landé-Edwards oxygenators, successfully treating 4 out of 13 patients (32).

HOLLOW FIBER OXYGENATORS BECOME STANDARD OF CARE: 1970s–PRESENT

The extracorporeal life support field began transitioning to the use of hollow fibers following the

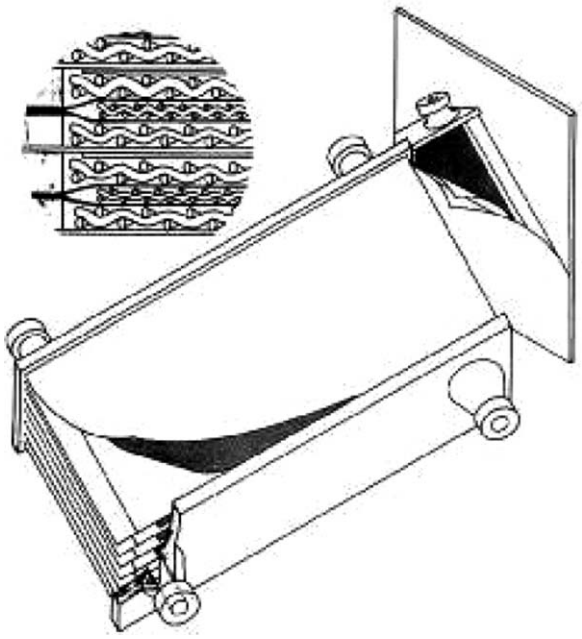

FIG. 5. Diagram showing the mesh support structure in the blood channels of the Travenol oxygenator, reproduced from Trudell (30). Mesh screens, shown in the inset, increased the total foreign material surface area in contact with blood, but interruption of blood flow induced turbulent mixing to enhance the rate of gas exchange and reduce the overall membrane area.

demonstrated success and wide availability of hollow fiber dialyzers for hemodialysis (33), with the first large-scale hollow fiber oxygenator reported in 1971 (11). Blood was routed through a manifold into the lumens of tens of thousands of hollow fibers with lengths of 10–18 cm; sweep gas flowed through a jacket surrounding the fibers, as shown in Fig. 6. Mathematical models of luminal flow hollow fiber oxygenators were developed during this time to guide the design of clinically relevant oxygenators (34,35).

Although luminal flow hollow fibers were theoretically capable of high gas exchange due to their circular cross section and correspondingly maximized surface to volume ratio, the 200–300 μm diameter lumen, lacking surface perturbations that could induce turbulent mixing, resulted in the formation of a plasma boundary layer in contact with the membrane surface, requiring longer fibers to ensure adequate diffusion of oxygen into the blood. The hydraulic resistance, which is inversely proportional to the fourth power of the fiber lumen diameter, also imposed large blood pressure drops across the oxygenator, risking hemolysis and requiring the use of powerful blood pumps.

Coagulation issues associated with silicone hollow fibers (36) were reduced and gas transport was greatly improved by the adoption of microporous polypropylene hollow fibers (37). The microporous structure provided open pores on the order of 1 μm in diameter for direct gas exchange between the sweep gas and blood (38), as shown in Fig. 7, without exposing red blood cells to the liquid-gas interface.

However, this introduced a new challenge of oxygenator wetting, in which blood plasma gradually infiltrated the micropores and greatly inhibited gas transfer. Several mechanisms were suspected of inducing pore wetting, including plasma evaporation and condensation in the cooler sweep gas (39), ultrafiltration of plasma through the micropores driven by high blood pressure (40), and wetting of micropores by phospholipids (41). Blood phospholipids bind non-specifically to the hollow fiber, creating a hydrophilic surface at the pore openings; plasma is then able to infiltrate the pore via capillary action, allowing phospholipids to bind further along the pore. The process continues until the entire pore is wetted and filled with plasma. The

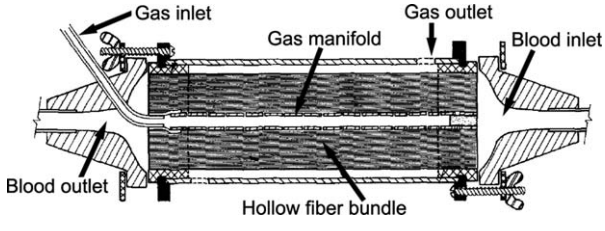

FIG. 6. Schematic of intraluminal blood flow hollow fiber oxygenator, adapted from Kaye (33). The high surface to volume ratio of the hollow fiber lumens allowed high gas exchange at the expense of high resistance to blood flow through individual fibers.

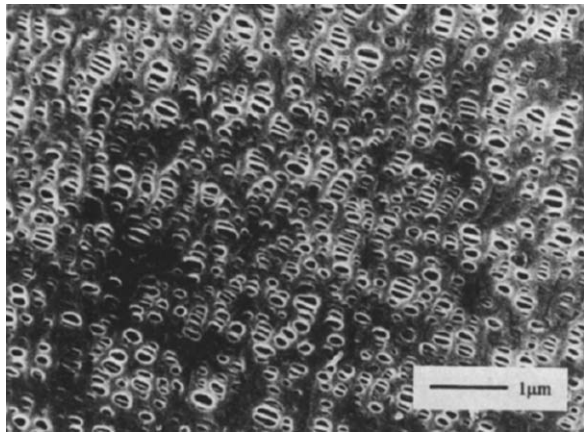

FIG. 7. Scanning electron micrograph of microporous surface of a single hollow fiber, reproduced from Kim (38). Open pores of less than 1 μm diameter form direct channels between the sweep gas and blood sides of the membrane.

much lower diffusivity of oxygen in water compared to air results in greatly diminished gas transfer across the membrane. Although increasing the sweep gas pressure can counteract plasma wetting, it risks introducing gas emboli into the blood stream. Consequently, plasma wetting eventually necessitates the replacement of the oxygenator and reconditioning the patient's blood to the new foreign surface.

Hydraulic resistance and boundary layer formation were overcome, not through the use of larger arrays of narrower fibers, but by employing "cross-flow" hollow fiber oxygenators (13). In this design, blood flowed outside of cross-woven hollow fibers while oxygen flowed in the fiber lumens, thereby providing a larger cross sectional area for blood flow and presenting a more chaotic blood path to induce mixing.

In order to address the plasma wetting issue, Kawahito and others explored the use of microporous hollow fibers skinned with silicone rubber (42–45). The hydrophobic silicone rubber prevented passage of water into the sweep gas channel; although purely diffusive transport of gas through the silicone diminished the rate of gas exchange, it was viewed as an acceptable tradeoff for increased oxygenator longevity.

The turn of the 21st century saw the introduction of a novel membrane material, polymethylpentene (PMP), which provided a microporous structure with a water-impermeable skin layer in contact with blood. This addressed the need to prevent plasma infiltration of pores, while presenting minimal resistance to diffusive transport of oxygen and carbon dioxide. Cross-flow hollow fiber oxygenators such as the Medos Hilite 7000LT (46) and Maquet Quadrox$_D$ (47) (shown in Fig. 8) were developed to bring PMP into clinical use.

The turbulent mixing and large cross-sectional area permitted by cross-flow hollow fiber oxygenators, allowing high blood flow at sub-100 mm Hg driving pressures, has also enabled a new class of specialized carbon dioxide removal devices. The Novalung interventional lung assist (iLA) (48) uses a PMP hollow fiber cartridge for pumpless extracorporeal carbon dioxide removal ($ECCO_2R$) in an arterio-venous blood circuit, while the ALung Hemolung RAS (49) utilizes an integrated centrifugal pump to drive blood through a fiber bundle and reduce fluid boundary layer thickness. Both systems provide oxygenation as well as carbon dioxide removal; however, the blood flows supported are approximately 1.5 L/min for the Novalung iLA and 0.5 L/min for the Hemolung, making them less suitable for full respiratory support.

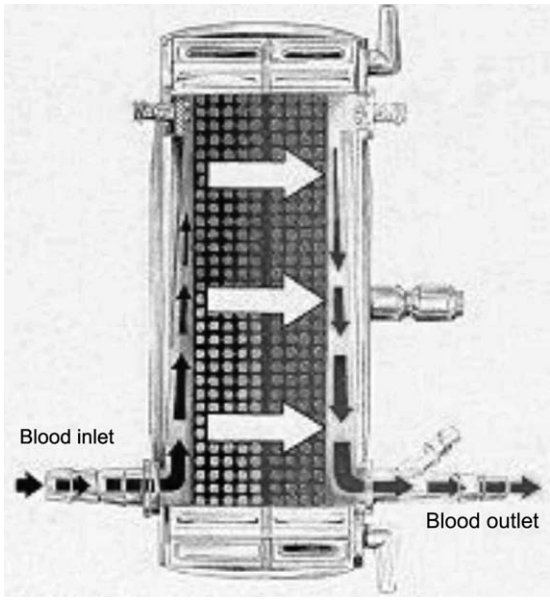

FIG. 8. Cross section of Maquet Quadrox oxygenator, illustrating cross flow of blood (white arrows) through mesh of hollow fibers oriented perpendicular to the blood flow path. Adapted from Horton et al. (47).

Hollow fiber oxygenators have become the standard of care for cardiopulmonary bypass and bedridden ECMO, with support of awake and ambulatory patients becoming increasingly common (50,51). However, improvements in reliability and ease of use are still needed to make ECMO feasible outside of specialized care centers. Despite the commercial use of immobilized heparin coatings on membrane surfaces (52), systemic anticoagulation is still necessary and increases the risk for bleeding, both internally and at cannulation sites. Oxygenator and circuit priming volumes in excess of 100 mL often require blood transfusions to initiate ECMO, especially for pediatric and neonatal patients. Additionally, the complex and fragile nature of the oxygenator and ECMO blood circuit make unassisted ambulatory ECMO a risky endeavor.

MICROFLUIDICS MIMIC NATIVE LUNGS: 1990s–FUTURE

In the native lung, red blood cells of approximately 8 μm diameter flow single-file through alveolar capillaries whose diameter can be as small as 3–5 μm, causing the red blood cells to deform and sweep along the capillary lumen (53). These tiny physical dimensions minimize the plasma layer through which oxygen must diffuse and permit

capillary lengths on the order of 1 mm. The geometry and manufacturing techniques used in hollow fiber oxygenators do not allow for such tight tolerances, with the result that their performance is limited by blood-side diffusive transport. However, the growing field of microfluidics (54) has inspired the use of soft lithography to define capillary blood channels for blood oxygenation.

Mockros and colleagues explored the theoretical benefits of microfluidic lungs to better mimic native lung physiology (14), concluding that parallel plates or large arrays of parallel capillary channels with critical blood channel dimensions approaching 10 μm would remove the majority of blood side resistance to gas diffusion, allowing the use of sub-1 cm blood flow path lengths and priming volumes below 50 mL to supply gas exchange needs for blood flows in excess of 4 L min^{-1}. Proof of concept was demonstrated using small-scale devices with 100 μm thick silicone rubber membranes mechanically supported by a 280 μm thick wire mesh spanning a 5 mm wide blood channel (55). Additional experiments demonstrated the feasibility of an open rectangular blood channel 15 μm high with a 130 μm thick membrane and integrated support columns fabricated from polydimethylsiloxane (PDMS) using soft lithography (56). This design indicated that arbitrarily wide blood channels were possible in a microfluidic device with a single critical dimension for gas transport—blood channel height—enabling oxygenators that were more tolerant of blood clots.

Burgess et al. fabricated monolithic PDMS membranes consisting of stacked arrays of parallel capillary channels with segmental cross sections. Each capillary channel had a maximum height of 33 μm, width of 105 μm, and length of 1.8 cm; gas exchange membranes tested were 64 or 146 μm thick (15). While the permeability to both oxygen and carbon dioxide was limited by the thickness of the membrane, it demonstrated the potential for PDMS-only capillary oxygenator arrays.

Potkay and colleagues expanded on the capillary array concept by using dramatically thinner 15 μm PDMS gas exchange membranes to enhance gas transfer (16,57–59); an example of this capillary channel geometry is shown in Fig. 9. Blood channels in these devices were 10–20 μm high, 88 μm wide, and less than 1 mm long. Meanwhile, Rochow et al. used PDMS to define the blood channels, testing both 6 μm thick microporous polycarbonate membranes or 20 μm thick PDMS for gas exchange. This enabled blood channels with 80 μm height and 500 μm width in a stackable design

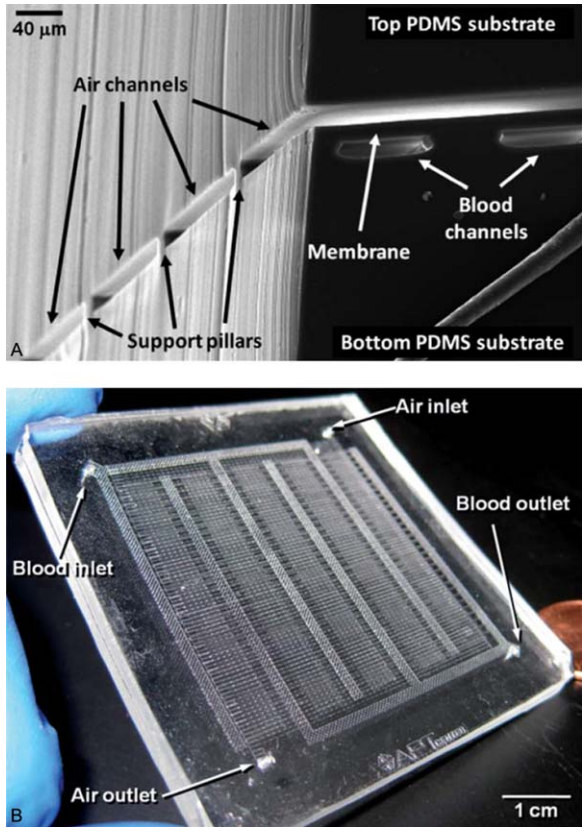

FIG. 9. Microfluidic artificial lung. (A) 15 μm tall blood channels and 20 μm thick gas exchange membrane fabricated from PDMS using soft lithography. (B) Array of capillary channels in a prototype oxygenator. Reproduced from Potkay (57). [Color figure can be viewed at wileyonlinelibrary.com]

(60–62). The high gas permeability of the thin PDMS membranes enabled the use of ambient air as a sweep gas, which could make dedicated pure oxygen supplies and gas mixers unnecessary.

Although individual capillary channels impose large resistance to blood flow, the use of thousands of capillaries in parallel works to overcome this effect; however, the manifolds at the blood inlet and outlet constitute the greatest source of hydraulic resistance (57). In order to control blood shear and minimize hydrodynamic pressure drop, especially at the blood inlet and outlet, recent work from the Potkay group and Draper Lab has focused on employing branching capillary channels that closely match the branching ratios found in the native lung (63–66); an example of this geometry is shown in Fig. 10. The <50 mm Hg pressure drop across optimized microfluidic systems could allow the use of smaller, less powerful blood pumps, or operate in a pumpless arterio-venous circuit.

Taken together, recent developments in microfluidic oxygenator designs make them a compelling

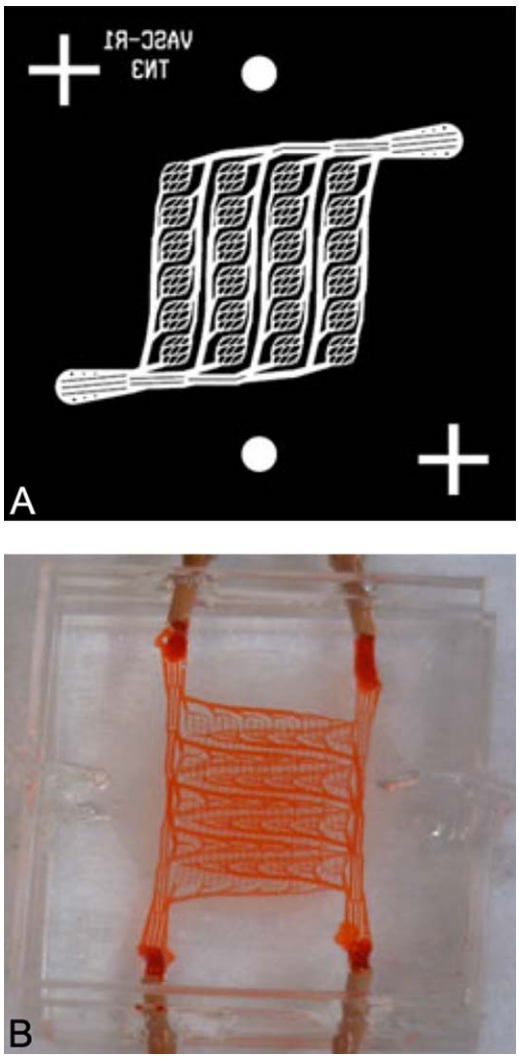

FIG. 10. (A) Schematic of biomimetic branching capillary design for a microfluidic lung, reproduced from Kniazeva (64). (B) Assembled stacked parallel plate microfluidic gas exchanger using branching capillaries, reproduced from Kniazeva (65). [Color figure can be viewed at wileyonlinelibrary.com]

avenue for further progress in ECMO technology toward compact, wearable systems that support unassisted ambulatory patients. However, the use of monolithic PDMS structures in recent designs could have detrimental consequences. Due to the hyperelastic mechanical properties of PDMS, capillary channels must be narrow in width (~500 μm or less) to avoid channel collapse or distension due to pressure differences between the sweep gas and blood. The side walls of each capillary do not contribute significantly to gas exchange, but add to the total surface area in direct contact with blood, making the narrow capillaries vulnerable to occlusion by clots (67).

A potential solution to these challenges could be found by combining the mechanically supported parallel plate geometry of Mockros et al. (55,56) with the sub-20 μm PDMS membranes of recent capillary oxygenators. An oxygenator incorporating these design features would benefit from the high gas permeability of plasma-impermeable solid membranes, the low blood side resistance of ~10 μm channel heights, and the greater clot tolerance of centimeter-scale channel widths. Such a system would in effect be an optimized version of the parallel plate oxygenators of the 1950s and 1960s.

CONCLUSION

As the evolution of extracorporeal membrane oxygenation continues, it is becoming possible to overcome past limitations of blood-side resistance to gas exchange. PDMS thin films can be produced at less than 20 μm thickness and greatly surpass the low permeability of early polymer membranes (16,57,61,62), and modern fabrication techniques can reliably produce defect-free membranes that minimize the risk of gas embolism (47). The stacked parallel plate blood channels used in the first clinical membrane oxygenators (24–28) can now be reproduced using soft lithography to yield sub-10 μm channel heights (56), significantly reducing plasma boundary layers. This approach allows for the use of shorter blood channel lengths with lower pressure drops and correspondingly decreased priming volume to more closely mimic the physiology of the native lungs. By revisiting membrane concepts and challenges from the 1950s and 1960s with state-of-the-art microfabrication technology, we are even closer to realizing a true artificial lung that can bridge the gap between sickness and health.

Acknowledgments: Funding for this work was provided by the Harry Wm. and Diana V. Hind Distinguished Professorship in Pharmaceutical Sciences II. The authors would like to thank Emily Abada and Ajay Dharia for valuable discussions and feedback.

Author Contributions: TY prepared the manuscript. SR provided critical feedback and secured funding.

Conflict of Interest: The authors have no conflicts of interest to disclose.

REFERENCES

1. Gaffney AM, Wildhirt SM, Griffin MJ, Annich GM, Radomski MW. Extracorporeal life support. *BMJ* 2010;341: 982–6.

2. Bartlett RH, Gattinoni L. Current status of extracorporeal life support (ECMO) for cardiopulmonary failure. *Minerva Anestesiol* 2010;76:534–40.
3. Toyoda Y, Bhama JK, Shigemura N, et al. Efficacy of extracorporeal membrane oxygenation as a bridge to lung transplantation. *J Thorac Cardiovasc Surg* 2013;145:1065–71.
4. Diaz-Guzman E, Hoopes CW, Zwischenberger JB. The evolution of extracorporeal life support as a bridge to lung transplantation. *ASAIO J* 2013;59:3–10.
5. Rehder KJ, Turner DA, Hartwig MG, et al. Active rehabilitation during extracorporeal membrane oxygenation as a bridge to lung transplantation. *Respir Care* 2013;58:1291–8.
6. Pruijsten R, van Thiel R, Hool S, Saeijs M. Mobilization of patients on venovenous extracorporeal membrane oxygenation support using an ECMO helmet. *Intensive Care Med* 2014;40:1595–7.
7. Gibbon JH. The development of the heart-lung apparatus. *Am J Surg* 1978;135:608–19.
8. Gibbon JH Jr. The application of a mechanical heart and lung apparatus to cardiac surgery. *Minn Med* 1954;37:171.
9. Clowes G Jr, Hopkins AL, Kolobow T. Oxygen diffusion through plastic films. *Trans Am Soc Artif Intern Organs* 1955;1:23–4.
10. Clowes GH Jr, Hopkins AL. Further studies with plastic films and their use in oxygenating blood. *Trans Am Soc Artif Intern Organs* 1956;2:6–12.
11. Dutton RC, Mather FW, III, Walker SN, Lipps BJ Jr. Development and evaluation of a new hollow-fiber membrane oxygenator. *Trans Am Soc Artif Intern Organs* 1971; 17:331–6.
12. Hill JD, O'Brien TG, Murray JJ, et al. Prolonged extracorporeal oxygenation for acute post-traumatic respiratory failure (shock-lung syndrome). Use of the Bramson membrane lung. *N Engl J Med* 1972;286:629–34.
13. Mockros LF, Leonard R. Compact cross-flow tubular oxygenators. *Trans Am Soc Artif Intern Organs* 1985;31:628–33.
14. Lee JK, Kung HH, Mockros LF. Microchannel technologies for artificial lungs: (1) theory. *ASAIO J* 2008;54:372–82.
15. Burgess KA, Hu H-H, Wagner WR, Federspiel WJ. Towards microfabricated biohybrid artificial lung modules for chronic respiratory support. *Biomed Microdevices* 2009; 11:117–27.
16. Potkay JA. A high efficiency micromachined artificial lung. *Transducers* 2009;2009:2234–7.
17. Kay EB, Berne RM, Zimmerman HA, Hirose Y. Experimental and clinical experience with a rotating disc oxygenator. *Trans Am Soc Artif Intern Organs* 1956;2:94–6.
18. Hagopian ER, Haupt GJ, Jr, JM, Templeton JY. A study of gas exchange in a stationary vertical screen oxygenator. *T Am Soc Art Int Org* 1961;7:157–61.
19. Ambrus JL. A simple heart-lung apparatus, not injurious to white cells or thrombocytes. *T Am Soc Art Int Org* 1955;1: 98–102.
20. Liddicoat JE, Bekassy SM, Beall AC, Jr. Membrane vs bubble oxygenator: clinical comparison. *Ann Surg* 1975;181: 747–52.
21. Dantowitz P, Borsanyi AS, Deibert MC, et al. A blood oxygenator with preformed membrane-lined, capillary channels. *T Am Soc Art Int Org* 1969;15:138.
22. Galletti PM. Applications of plastics in membrane oxygenators. *J Biomed Mater Res* 1971;5:129–34.
23. Kolobow T, Bowman RL. Construction and evaluation of an alveolar membrane artificial heart-lung. *Trans Am Soc Artif Intern Organs* 1963;9:238–43.
24. Bramson ML, Osborn JJ, Main FB, O'Brien MF, Wright JS, Gerbode F. A new disposable membrane oxygenator with integral heat exchanger. *J Thorac Cardiovasc Surg* 1965;50:391–400.
25. Schulte HD. First steps in membrane oxygenation and prolonged extracorporeal perfusion in Duesseldorf using the Bramson membrane lung. *Perfusion* 2003;18:185–9.
26. Landé AJ, Parker B, Carlson V, Lillehei CW. Methods for increasing the efficiency of a new dialyzer-membrane oxygenator. *Trans Am Soc Artif Intern Organs* 1968;14: 227–32.
27. Landé AJ, Edwards L, Bloch JH, et al. Clinical experience with emergency use of prolonged cardiopulmonary bypass with a membrane pump-oxygenator. *Ann Thorac Surg* 1970; 10:409–23.
28. Carlson RG, Landé AJ, Ivey LA, et al. The Landé-Edwards disposable plastic membrane oxygenator for total and partial cardiopulmonary support during aortocoronary artery-vein graft operations. *Eur Surg Res* 1972;4:393–406.
29. Gaylor J, Mockros LF. Artificial-lung design: sheet-membrane units. *Med Biol Eng* 1975;13:425–35.
30. Trudell LA, Friedman LI, Kakvan M, Galletti PM. Evaluation of a disposable membrane oxygenator. *Trans Am Soc Artif Intern Organs* 1972;18:538–45.
31. Kolobow T, Borelli M, Spatola R. Artificial lung (oxygenators). *Artif Organs* 1986;10:370–7.
32. Bartlett RH, Gazzaniga AB, Jefferies MR, Huxtable RF, Haiduc NJ, Fong SW. Extracorporeal membrane oxygenation (ECMO) cardiopulmonary support in infancy. *Trans Am Soc Artif Intern Organs* 1976;22:80–93.
33. Kaye MP, Pace JB, Blatt SJ, Ferguson GS. Use of a capillary membrane oxygenator for total cardiopulmonary bypass in calves. *J Surg Res* 1973;14:58–63.
34. Buckles RG, Merrill EW, Gilliland ER. An analysis of oxygen absorption in a tubular membrane oxygenator. *AIChE J* 1968;14:703–8.
35. Mockros LF, Gaylor J. Artificial lung design: tubular membrane units. *Med Biol Eng* 1975;13:171–81.
36. Dutton RC, Edmunds LH. Formation of platelet aggregate emboli in a prototype hollow fiber membrane oxygenator. *J Biomed Mater Res* 1974;8:163–83.
37. Suma K, Tsuji T, Takeuchi Y, Inoue K, Shiroma K. Clinical performance of microporous polypropylene hollow-fiber oxygenator. *Ann Thorac Surg* 1981;32:558–62.
38. Kim JJ, Jang TS, Kwon YD, Kim UY, Kim SS. Structural study of microporous polypropylene hollow fiber membranes made by the melt-spinning and cold-stretching method. *J Memb Sci* 1994;93:209–15.
39. Mottaghy K, Oedekoven B, Starmans H, et al. Technical aspects of plasma leakage prevention in microporous capillary membrane oxygenators. *Trans Am Soc Artif Intern Organs* 1989;35:640–3.
40. Tamari Y, Tortolani AJ, Maquine M, Lee-Sensiba K, Guarino J. The effect of high pressure on microporous membrane oxygenator failure. *Artif Organs* 1991;15:15–22.
41. Montoya JP, Shanley CJ, Merz SI, Bartlett RH. Plasma Leakage through microporous membranes: role of phospholipids. *ASAIO J* 1992;38:M399–405.
42. Shimono T, Shomura Y, Hioki I, Shimamoto A. Silicone-coated polypropylene hollow-fiber oxygenator: experimental evaluation and preliminary clinical use. *Ann Thorac Surg* 1997;63:1730–6.
43. Kawahito S, Maeda T, Motomura T, et al. Development of a new hollow fiber silicone membrane oxygenator: in vitro study. *Artif Organs* 2001;25:494–8.
44. Kawahito S, Motomura T, Glueck J, Nosé Y. Development of a new hollow fiber silicone membrane oxygenator for ECMO: the recent progress. *Ann Thorac Cardiovasc* 2002;8: 268–74.
45. Eash HJ, Jones HM, Hattler BG, Federspiel WJ. Evaluation of plasma resistant hollow fiber membranes for artificial lungs. *ASAIO J* 2004;50:491–7.
46. Peek GJ, Killer HM, Reeves R, Sosnowski AW, Firmin RK. Early experience with a polymethyl pentene oxygenator for adult extracorporeal life support. *ASAIO J* 2002;48:480–2.
47. Horton S, Thuys C, Bennett M, Augustin S, Rosenberg M, Brizard C. Experience with the Jostra Rotaflow and QuadroxD oxygenator for ECMO. *Perfusion* 2004;19:17–23.

48. Bartosik W, Egan JJ, Wood AE. The Novalung interventional lung assist as bridge to lung transplantation for self-ventilating patients—initial experience. *Interact Cardiovasc Thorac Surg* 2011;13:198–200.
49. Batchinsky AI, Jordan BS, Regn D, et al. Respiratory dialysis: reduction in dependence on mechanical ventilation by venovenous extracorporeal CO2 removal. *Crit Care Med* 2011;39:1382–7.
50. Turner DA, Cheifetz IM, Rehder KJ, et al. Active rehabilitation and physical therapy during extracorporeal membrane oxygenation while awaiting lung transplantation: a practical approach. *Crit Care Med* 2011;39:2593–8.
51. Garcia JP, Kon ZN, Evans C, et al. Ambulatory veno-venous extracorporeal membrane oxygenation: innovation and pitfalls. *J Thorac Cardiovasc Surg* 2011;142:755–61.
52. Preston TJ, Ratliff TM, Gomez D. Modified surface coatings and their effect on drug adsorption within the extracorporeal life support circuit. *J Extra Corpor Technol* 2010;42: 199–202.
53. Hellums JD, Nair PK, Huang NS, Ohshima N. Simulation of intraluminal gas transport processes in the microcirculation. *Ann Biomed Eng* 1996;24:1–24.
54. Duffy DC, McDonald JC, Schueller OJA, Whitesides GM. Rapid prototyping of microfluidic systems in poly(dimethylsiloxane). *Anal Chem* 1998;70:4974–84.
55. Kung MC, Lee JK, Kung HH, Mockros LF. Microchannel technologies for artificial lungs: (2) screen-filled wide rectangular channels. *ASAIO J* 2008;54:383–9.
56. Lee JK, Kung MC, Kung HH, Mockros LF. Microchannel technologies for artificial lungs: (3) open rectangular channels. *ASAIO J* 2008;54:390–5.
57. Potkay JA, Magnetta M, Vinson A, Cmolik B. Bio-inspired, efficient, artificial lung employing air as the ventilating gas. *Lab Chip* 2011;11:2901–9.
58. Potkay JA. A simple, closed-form, mathematical model for gas exchange in microchannel artificial lungs. *Biomed Microdevices* 2013;15:397–406.
59. Potkay JA. The promise of microfluidic artificial lungs. *Lab Chip* 2014;14:4122–38.
60. Rochow N, Wu W-I, Chan E, et al. Integrated microfluidic oxygenator bundles for blood gas exchange in premature infants. *MEMS* 2012;2012:957–60.
61. Wu W-I, Rochow N, Chan E, et al. Lung assist device: development of microfluidic oxygenators for preterm infants with respiratory failure. *Lab Chip* 2013;13:2641.
62. Rochow N, Manan A, Wu W-I, et al. An integrated array of microfluidic oxygenators as a neonatal lung assist device: in vitro characterization and in vivo demonstration. *Artif Organs* 2014;38:856–66.
63. Kovach KM, LaBarbera MA, Moyer MC, et al. In vitro evaluation and in vivo demonstration of a biomimetic, hemocompatible, microfluidic artificial lung. *Lab Chip* 2015; 15:1366–75.
64. Kniazeva T, Hsiao JC, Charest JL, Borenstein JT. A microfluidic respiratory assist device with high gas permeance for artificial lung applications. *Biomed Microdevices* 2011;13: 315–23.
65. Kniazeva T, Epshteyn AA, Hsiao JC, et al. Performance and scaling effects in a multilayer microfluidic extracorporeal lung oxygenation device. *Lab Chip* 2012;12:1686–95.
66. Hoganson DM, Anderson JL, Weinberg EF, et al. Branched vascular network architecture: a new approach to lung assist device technology. *J Thorac Cardiovasc Surg* 2010;140:990–5.
67. Kovach KM, Capadona JR, Gupta Sen A, Potkay JA. The effects of PEG-based surface modification of PDMS microchannels on long-term hemocompatibility. *J Biomed Mater Res A* 2014;102:4195–205.